

Signatures of quasi-Dirac neutrinos in diffuse high-energy astrophysical neutrino data

Kiara Carloni,^{1,*} Yago Porto,^{2,3,†} Carlos A. Argüelles,^{1,‡} P. S. Bhupal Dev,^{4,§} and Sudip Jana^{5,¶}

¹*Department of Physics & Laboratory for Particle Physics and Cosmology,
Harvard University, Cambridge, MA 02138, USA*

²*Centro de Ciências Naturais e Humanas, Universidade Federal do ABC, 09210-170, Santo André, SP, Brazil*

³*Instituto de Física Gleb Wataghin, Universidade Estadual de Campinas, 13083-859, Campinas, SP, Brazil*

⁴*Department of Physics and McDonnell Center for the Space Sciences,
Washington University, St. Louis, MO 63130, USA*

⁵*Harish-Chandra Research Institute, A CI of Homi Bhabha National Institute,
Chhatnag Road, Jhansi, Prayagraj 211 019, India*

We search for signatures of extremely long-baseline oscillations between left- and right-handed neutrinos using the high-energy astrophysical neutrino spectra measured by IceCube. We assume the astrophysical neutrino sources to be distributed in redshift following the star formation rate and use the IceCube all-sky flux measurements from TeV to PeV energies. We find, for the first time, that δm^2 in the range 2×10^{-19} to $3 \times 10^{-18} \text{eV}^2$ is disfavored at the 3σ confidence level, while there exists a preference for a δm^2 of $1.9 \times 10^{-19} \text{eV}^2$ at 2.8σ . This preference for quasi-Dirac neutrinos is driven by the tension between cascade and track measurements below 30 TeV.

Introduction.— The observation of solar neutrinos played a pivotal role in the discovery of nonzero neutrino masses and mixing. As we will argue in this Letter, the study of high-energy astrophysical neutrinos can similarly provide new insights into the nature of neutrino masses.

The fundamental origin of neutrino oscillations and the precise nature of neutrino mass remain unknown. Currently, the best bet we have to resolve the Dirac versus Majorana nature of neutrinos is via the neutrinoless double beta decay ($0\nu\beta\beta$) process [1]. However, there is no guarantee that even next-generation ton-scale $0\nu\beta\beta$ experiments may yield a positive signal if neutrino masses follow the normal ordering, a scenario that is mildly favored by current global oscillation fits [2]. On the other hand, the traditional oscillation-based neutrino experiments are only sensitive to the squared mass differences and do not alter chirality; hence, they cannot resolve the distinction between Dirac and Majorana neutrinos. In contrast, as we will show below, the oscillations of high-energy neutrinos over astrophysical baselines provide a unique opportunity to probe extremely small squared mass differences, and hence, a whole class of neutrino mass models featuring tiny lepton number breaking.

The most important open question in neutrino physics is how neutrinos get their mass [3]. One possible answer is that neutrinos acquire their mass in the same way the charged fermions do, through a Dirac mass term originating from a Yukawa coupling to the Higgs field. However, such a term would require the introduction of new, right-handed neutrino fields, ν_R , which, being singlets under the Standard Model (SM) gauge group, allow for a Majorana mass term, $\frac{1}{2}m_R\bar{\nu}_R^c\nu_R$, where $\bar{\nu}_R^c \equiv \nu_R^T C^{-1}$, with C being the charge conjugation operator. Since the Majorana mass m_R is unconstrained in a bottom-up phenomenological approach, it is theoretically allowed to be much smaller than the original Dirac mass term [4–8].

This scenario produces what are called quasi-Dirac neutrinos or, for short, *QDinos* (pronounced /'kjʊ:di:nous/), and will be the focus of this Letter.

The only experimental way to directly probe QDinos is by searching for oscillations in the spectra of neutrinos from astrophysical sources, such as the Sun [11–17], supernovae [9, 18], high-energy cosmic sources [10, 19–

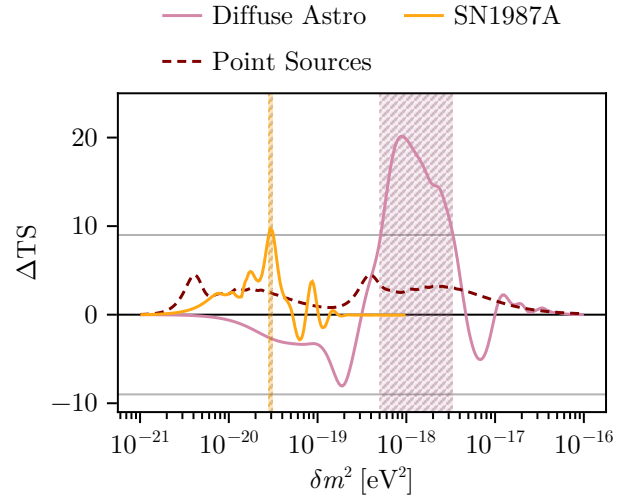


FIG. 1. **Constraints on the QDino parameter space.** The test statistic difference with respect to the null hypothesis, from our current analysis, is plotted in light purple as a function of the QDino mass-squared difference (δm^2). Regions with positive ΔTS are disfavored with respect to the null; negative are favored. Grey horizontal lines indicate the 3σ threshold according to Wilks’ theorem with 1 degree of freedom. In yellow we plot the constraints obtained using SN1987A data in Ref. [9]. In dashed dark purple we show the sensitivity with point sources at IceCube obtained in Ref. [10].

29], or relic neutrinos [30]. These oscillations are driven by the hyperfine mass-squared difference, $\delta m_k^2 \propto m_R$. Stringent upper limits on $\delta m_{1,2}^2 \lesssim 10^{-12} \text{eV}^2$ have been derived using solar neutrinos [13, 16]. The solar limit supercedes a previously derived constraint from Big Bang Nucleosynthesis (BBN), $\delta m_i^2 \lesssim 10^{-8} \text{eV}^2$ [31, 32]. These limits are derived assuming maximal active-sterile neutrino mixing in the QDino scenario. If the mixing is non-maximal, the δm^2 limits can be much weaker [16, 33]. Moreover, the solar neutrino data is not sensitive to δm_3^2 due to the small electron component in ν_3 , and the limits from atmospheric, accelerator and reactor neutrino data are too weak, $\delta m_3^2 \lesssim 10^{-5} \text{eV}^2$ [14], due to the much shorter baselines.

The identification of a few point sources of astrophysical neutrinos [34] provides sensitivity to QDinos with $\delta m_i^2 \in [10^{-21}, 10^{-16}] \text{eV}^2$ [10]; see also Refs. [35, 36] for related analyses. However, the current prospective for exploring the QDino parameter space in this mass range using point sources is limited by the small numbers of identified sources, the poor energy resolution for measuring muon neutrinos, and the lack of flavor information. These problems do not allow high-significance statements about QDinos at present.

In this work, for the first time, we use the diffuse astrophysical neutrino flux measured by IceCube in multiple channels and flavors, to explore QDinos in the mass-squared difference range of $\delta m_i^2 \in [10^{-21}, 10^{-16}] \text{eV}^2$. This strategy has two advantages over point-source based analyses: firstly, measurements in multiple channels with different flavor combinations are available, and secondly, the astrophysical neutrino sample size is much larger. The downside of a diffuse flux analysis is that the oscillation probability is smeared out by the spatial distribution of astrophysical neutrino sources, which is unknown.

Diffuse astrophysical neutrinos were first observed using the High-Energy Starting Events (HESE) dataset, which includes neutrinos of all flavors and directions with energies greater than 60 TeV and is well-described by a single power-law (SPL) energy spectrum [37–39], $E^{-\gamma}$. These first measurements of the diffuse flux have been extended to lower energies using electron and tau neutrino-dominated samples [40–42], as well as samples of muon neutrinos interacting within the detector volume [43], and have been complemented at higher energies by samples of muon neutrinos [44–46]. The spectral measurements of these analyses are all consistent with $\gamma = 2.5$ between 30 TeV and 200 TeV [43], but at either end, tensions exist between samples dominated by different flavors. For example, the electron and tau neutrino-dominated sample found a hardening of the spectra at low energies, $\gamma_{\text{low}} = 2.11_{-0.67}^{+0.29}$ [42], while the most recent muon neutrino sample prefers a softer spectrum $\gamma_{\text{low}} = 2.79_{-0.5}^{+0.3}$ [43].

In this Letter, we show that the region where the spectral measurements in different flavors are consistent al-

lows us to place the first significant constraints on the QDino mass-squared difference δm^2 around 10^{-18}eV^2 , see Fig. 1. Additionally, we point out for the first time that the tensions at low energies can also be explained by QDinos [47].

Theory of quasi-Dirac neutrinos.— It is unknown whether the neutrino mass term is Majorana, Dirac, or a mixture of both [4, 5]. In particular, if the Majorana mass term is much smaller than the Dirac, neutrinos are *QDinos* [6–8], which are fundamentally Majorana fermions but behave like Dirac in most experimental settings. In the QDino scenario, lepton number is only slightly violated, and lepton number violating observables such as $0\nu\beta\beta$ are strongly suppressed. Ordinary neutrinos have three generations of mass states, ν_i , whose decomposition into flavor states, ν_α , is described by the PMNS matrix. If neutrinos are QDinos, each generation has a further hyper-fine mass splitting, δm_i^2 , which produces two mass states per generation, ν_i^\pm , which are orthogonal equal combinations of active (LH) and sterile (RH) states. In the same way that ordinary neutrinos undergo flavor oscillations after traveling distances $L \sim E/\Delta m^2$, QDinos undergo active-sterile oscillations over much longer distances $L \sim E/\delta m^2$, where E is the neutrino energy. These ultra-long baseline oscillations are the only distinguishing signature of QDinos.

The theoretical and model-building aspects of QDinos have been extensively discussed in the literature; see e.g., Refs. [10, 13, 25, 50–58]. It is interesting to note that certain string theory landscape constructions, such as Swampland, predict that neutrinos are Dirac-like particles [59–62]. Additionally, we expect that global symmetries such as lepton number are ultimately broken by quantum gravity, turning Dirac neutrinos into QDinos. In fact, any model where neutrinos start as Dirac particles with conserved lepton number could receive non-renormalizable quantum gravity corrections which generate small δm^2 via higher-dimensional lepton-number-violating operators suppressed by the Planck scale, thus making neutrinos naturally QDinos. QDinos could also help explain some features of astrophysical and cosmological observations. For example, small δm^2 values could also be linked to the observed baryon asymmetry of the Universe [57, 63]. QDinos have also been suggested as solutions to the excess in the diffuse radio background [64, 65].

Quasi-Dirac oscillations on astrophysical scales.— The QDino nature of neutrinos modifies standard flavor oscillations by introducing additional frequencies beyond those associated with the “solar” ($\Delta m_{21}^2 \approx 7.5 \times 10^{-5} \text{eV}^2$) and “atmospheric” ($\Delta m_{31}^2 \approx 2.5 \times 10^{-3} \text{eV}^2$) mass-squared differences. These new oscillation components convert active neutrino mass eigenstates, ν_k , into their sterile counterparts with frequencies proportional to δm_k^2 .

For any combination of neutrino energy, E , and prop-

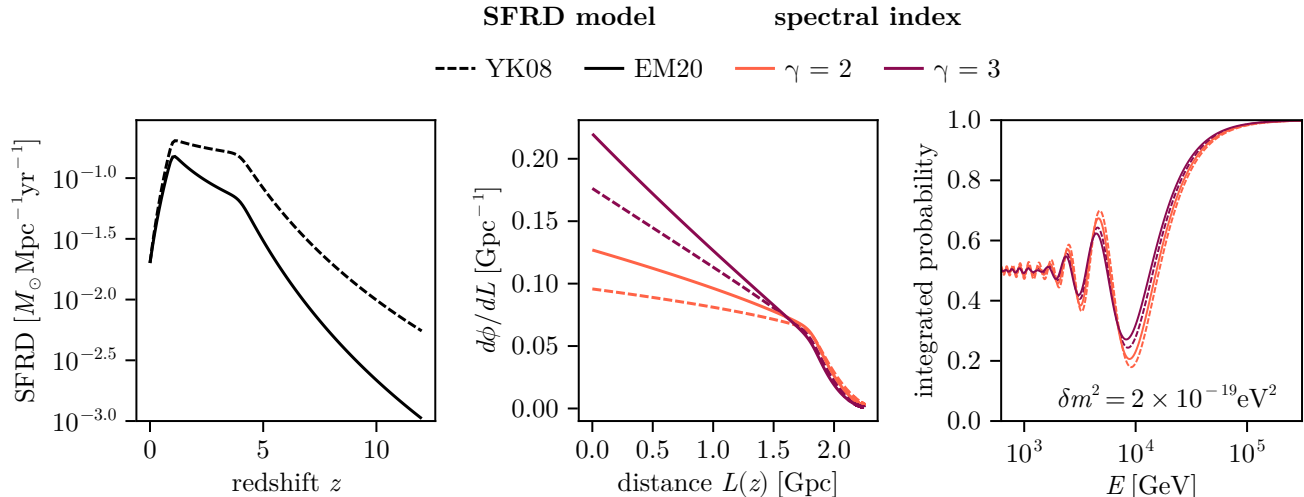


FIG. 2. **Source distribution and integrated oscillation probability.** *Left:* SFRD distributions as a function of redshift for two different star formation models discussed in Refs. [48, 49]. *Middle:* Distribution of the diffuse neutrino flux over the effective distance (L_{eff}) between emission and detection, assuming a given SFRD model and spectral index. *Right:* QDino survival probability as a function of detected neutrino energy, integrated over the distance distribution.

agation distance, L , suitable for probing allowed QDino mass squared differences, δm^2 , the standard oscillation terms containing Δm^2 will average out due to limited experimental resolution. In this regime, the oscillation probability is given by

$$P_{\alpha\beta} = \frac{1}{2} \sum_{k=1}^3 |U_{\beta k}^* U_{\alpha k}|^2 \left[1 + \cos \left(\frac{\delta m_k^2 L_{\text{eff}}}{2E} \right) \right]. \quad (1)$$

Here, E is the neutrino energy as measured on Earth, and

$$L_{\text{eff}} = \int \frac{dz}{H(z)(1+z)^2}, \quad (2)$$

is the effective oscillation distance, that accounts for neutrino propagation in an expanding Universe and depends on the Hubble expansion rate, $H(z)$. See [66] for a discussion about decoherence effects.

The diffuse neutrino flux is produced by a population of sources distributed across cosmological time and space. Without specifying the exact nature of these sources, we assume that their distribution follows the star formation rate density (SFRD) [48, 49], denoted by $\dot{\rho}_*(z)$; see the left panel of Fig. 2. In this scenario, the number of neutrino sources within a redshift interval $[z, z+dz]$ is given by

$$dN(z) \propto \dot{\rho}_*(z) \times 4\pi D^2 \frac{dD}{dz} dz, \quad (3)$$

where $D(z) = \int \frac{dz}{H(z)}$ is the comoving distance. We as-

sume that each source at redshift z emits a neutrino flux of the form $\phi_\alpha(E_z) = f_\alpha \phi^0 (E_z/E_0)^{-\gamma}$ for a given flavor α , where E_z is the energy at the source, $E_z = E(1+z)$, f_α is the fraction of the flavor α , and ϕ^0 is the flux at E_0 . Including QDino oscillations, the contribution to the total diffuse flux from a given redshift interval is

$$d\Phi_\beta(z, E) = \sum_{\alpha} P_{\alpha\beta}(z, E) \phi_\alpha(z, E) dN(z). \quad (4)$$

The total flux at Earth as a function of energy is therefore given by

$$\Phi_\beta(E) \propto \int \sum_{\alpha} P_{\alpha\beta}(z, E) \times \dot{\rho}_*(z) \times f_\alpha \phi^0 \left(\frac{E(1+z)}{E_0} \right)^{-\gamma} \frac{dz}{H(z)}. \quad (5)$$

The total diffuse flux is dominated by the contributions of sources at $z \leq 1$, as shown in the middle panel of Fig. 2. Since the source distribution has a dominant scale, QDino oscillations are not completely averaged out when integrating $P_{\alpha\beta}$ over the source distribution (right panel of Fig. 2).

Analysis.— IceCube analyses typically classify neutrino events into two morphologies, cascades and tracks, composed of different combinations of flavors. Track events are dominated by muon neutrinos, with a subdominant contribution from tau neutrinos, while cascade events are comprised of all flavors, since electromagnetic and hadronic showers cannot be differentiated

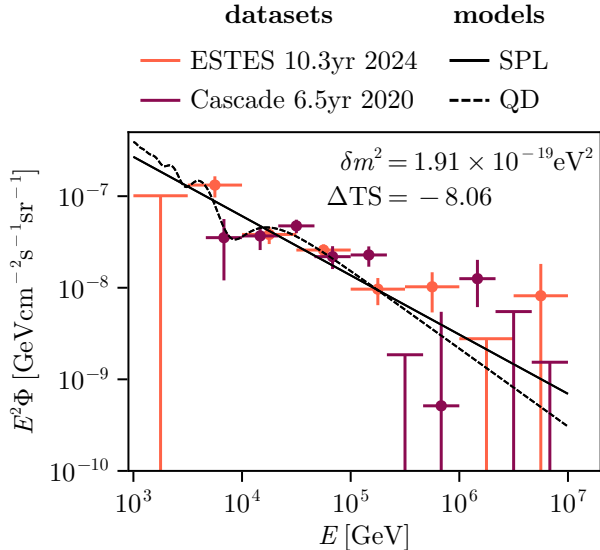


FIG. 3. *Flux predictions and IceCube measurements.* The best-fit QDino flux hypothesis (black, dashed) and no QDino hypothesis (black, solid), plotted along with the piecewise per-flavor flux normalizations reported by the **CASCADE** and **ESTES** IceCube analyses. The ΔTS stated is the difference between these two fits.

in IceCube. In our analysis, we use two statistically independent datasets, which select events with different morphologies. The **CASCADE** sample [42] is a selection of cascade events collected over 6.5 years of data-taking. The **ESTES** sample [43] is a selection of muon neutrinos which interact in the detector volume (“starting tracks”) collected over 10.3 years of data-taking. Both analyses have been used to extract the astrophysical neutrino flux, reported as a piece-wise E^{-2} flux assuming equal flavor at Earth. For each sample, we will use the published detector efficiencies to compare our predictions, including QDino oscillations, with the extracted fluxes.

The reported piecewise flux normalizations, Φ_i^S , can be converted into an approximate number of astrophysical neutrinos per bin N_i in the following way:

$$N_i^S = \Delta T^S \int_{E_i}^{E_{i+1}} dE \left[E^{-2} \Phi_i^S \sum_{\alpha} A_{\alpha}^S(E) \right], \quad (6)$$

where ΔT^S is the total livetime of the sample S , and A_{α}^S is the flavor-dependent, zenith-averaged effective area of the sample. Additionally, we convert the total uncertainties (statistical and systematic) on the reported flux normalizations into uncertainties σ_i^S on N_i^S . Similarly, we can compute the expected number of events in a bin, $\mu_i^S(\delta m_k^2, \vec{\eta})$ according to an astrophysical flux model $\Phi_{\alpha}(E|\delta m_k^2, \vec{\eta})$ using the effective areas. The flux $\Phi_{\alpha}(E)$ depends on the QDino parameters δm_k^2 , as well

as on the source flavor ratio, normalization, and spectral index, which we collectively denote as the flux parameters $\vec{\eta}$. We report results assuming that the initial flavor ratio is that of pion decay, $f_{\alpha} = (1, 2, 0)$, since muon-damped and neutron-decay yield similar exclusions but less-favored preferred regions. We assume that the redshift distribution of sources is proportional to the star formation rate density model from Ref. [49], and use Eq. (5) to calculate the averaged oscillation probability.

To determine preferred and excluded regions of δm^2 parameter space, relative to the non-QDino hypothesis, we use the following test statistic:

$$TS(\delta m_k^2) = \min_{\vec{\eta}} \sum_S \sum_i (N_i^S - \mu_i^S(\delta m_k^2, \vec{\eta}))^2 / (\sigma_i^S)^2. \quad (7)$$

Assuming Wilks’ theorem, we construct our confidence regions by assuming that the difference $\Delta TS(\delta m_k^2) = TS(\delta m_k^2) - TS(0)$, with the appropriate sign for preference or exclusion, follows a χ^2 distribution.

Results.— Assuming a single mass-squared difference for all three generations, $\delta m_k^2 = \delta m^2$, we find that the reported astrophysical fluxes excludes $\delta m^2 \in [5 \times 10^{-19}, 3 \times 10^{-18}] \text{ eV}^2$ at the 3σ level (red curve in Fig. 1). This is because the reported data is well-described by an unbroken power law in the energy range approximately between 10^4 to 10^5 GeV. The constraints that we obtain in this model are stronger than those obtained from SN1987A neutrino data [9], shown in yellow in Fig. 1. We find a preference for $\delta m^2 = 1.9 \times 10^{-19} \text{ eV}^2$ at a significance of 2.8σ , and a milder preference for $\delta m^2 = 6.5 \times 10^{-18} \text{ eV}^2$, see Table I. These preferences are driven by two distinct features in the energy distributions of the two samples. The larger preference, at the smaller δm^2 , is driven by the deficit in the **CASCADE** sample below 30 TeV compared to **ESTES**. This best-fit flux is displayed as the dashed black curve in Fig. 3. The smaller preference is caused by the lack of events in the **CASCADE** sample around 300 TeV. We note that both preferences for a QDino scenario are based on spectral effects only, which are distinguishable because the two datasets report their results with different choices of energy binning. The significance of this result is therefore reliant on the assumptions on the underlying astrophysical spectra, i.e. a power-law.

In contrast, when we allow for two distinct mass-squared differences, $\delta m_i^2 \neq \delta m_{j,k}^2$, the QDino model produces observable effects in both energy and flavor. Since in the absence of new physics, astrophysical neutrinos are expected to arrive in equal flavors (assuming standard pion and muon decays at source), any flavor ratio effect is very robust under spectral modeling. In this case, we find that a region of parameter space is also disfavored at the same significance. This result is driven by both the power-law shape of the energy distribution in the range 10^4 to 10^5 GeV, and the consistency of the two samples in this range. In this scenario, the best-fit point has a

similar test-statistic difference as in the 1-parameter scenario (see Table I), with a similar parameter value, but the significance is reduced due to the increased degree of freedom. The allowed and disfavored parameter space for $\delta m_1^2 \neq \delta m_{2,3}^2$ is shown in Suppl. Fig. 1.

$\delta m_1^2[\text{eV}^2]$	$\delta m_2^2[\text{eV}^2]$	$\delta m_3^2[\text{eV}^2]$	DOF	ΔTS
1.9×10^{-19}	δm_1^2	δm_1^2	1	-8.06
1.6×10^{-19}	2.0×10^{-19}	δm_2^2	2	-8.16
2.0×10^{-19}	2.0×10^{-19}	δm_1^2	2	-7.91
1.6×10^{-19}	δm_1^2	2.5×10^{-19}	2	-8.11

TABLE I. Best-fit QDino model parameters, for varying choices of δm_k^2 . See supplemental material for more details.

Conclusions. — Neutrino telescopes provide a unique opportunity to study the properties of QDinos (Quasi-Dirac neutrinos). In this Letter, assuming the distribution of astrophysical neutrino sources to follow the star formation rate, we have shown that QDino oscillations lead to observable effects in both the spectrum and flavor composition of astrophysical neutrinos. We use the reported astrophysical neutrino flux of two IceCube event selections, CASCADE and ESTES, which have distinct flavor compositions, to probe the QDino parameter space. We obtain the first significant constraint for QDinos with mass-splittings smaller than 10^{-12}eV^2 . We disfavor, at the 3σ level, mass-squared differences between $[5 \times 10^{-19}, 3 \times 10^{-18}]\text{eV}^2$.

Additionally, we find that the existence of $\delta m^2 = 1.9 \times 10^{-19} \text{eV}^2$ can alleviate the observed tension between the cascade and track samples by 2.8σ . We find a secondary preference for $\delta m^2 = 6.5 \times 10^{-18}\text{eV}^2$, driven by the persistent deficit of cascade events at 300 TeV. This new explanation of these spectral features is potentially testable in future observations of the diffuse flux or of point source spectra. Upcoming IceCube analyses, leveraging more years of existing data, could confirm or refute this tension. On a longer timescale, measurements by water-Cherenkov telescopes (such as KM3NeT) can provide independent confirmation.

Acknowledgments. — We thank Subir Sarkar for useful comments on the draft. KC is supported by the NSF Graduate Research Fellowship under Grant No. 2140743, and the Research Corporation for Science Advancement Cottrell Scholar award. The work of YP was supported by the São Paulo Research Foundation (FAPESP) Grant No. 2023/10734-3 and 2023/01467-1, and by the National Council for Scientific and Technological Development (CNPq) Grant No. 151168/2023-7. CAA are supported by the Faculty of Arts and Sciences of Harvard University, the National Science Foundation, the Research Corporation for Science Advancement, and the David & Lucile Packard Foundation. The work of

BD is partly supported by the U.S. Department of Energy under grant No. DE-SC0017987. SJ would like to acknowledge support from the Department of Atomic Energy, Government of India, for the Harish-Chandra Research Institute.

* kcarloni@g.harvard.edu
 † yago.porto@ufabc.edu.br
 ‡ carguelles@fas.harvard.edu
 § bdev@wustl.edu
 ¶ hep.sudip@gmail.com

- [1] M. Agostini, G. Benato, J. A. Detwiler, J. Menéndez, and F. Vissani, Toward the discovery of matter creation with neutrinoless $\beta\beta$ decay, *Rev. Mod. Phys.* **95**, 025002 (2023), [arXiv:2202.01787 \[hep-ex\]](https://arxiv.org/abs/2202.01787).
- [2] I. Esteban, M. C. Gonzalez-Garcia, M. Maltoni, I. Martinez-Soler, J. a. P. Pinheiro, and T. Schwetz, NuFit-6.0: updated global analysis of three-flavor neutrino oscillations, *JHEP* **12**, 216, [arXiv:2410.05380 \[hep-ph\]](https://arxiv.org/abs/2410.05380).
- [3] R. N. Mohapatra *et al.*, Theory of neutrinos: A White paper, *Rept. Prog. Phys.* **70**, 1757 (2007), [arXiv:hep-ph/0510213](https://arxiv.org/abs/hep-ph/0510213).
- [4] L. Wolfenstein, Different Varieties of Massive Dirac Neutrinos, *Nucl. Phys. B* **186**, 147 (1981).
- [5] S. T. Petcov, On Pseudodirac Neutrinos, Neutrino Oscillations and Neutrinoless Double beta Decay, *Phys. Lett. B* **110**, 245 (1982).
- [6] J. W. F. Valle and M. Singer, Lepton Number Violation With Quasi Dirac Neutrinos, *Phys. Rev. D* **28**, 540 (1983).
- [7] M. Doi, M. Kenmoku, T. Kotani, H. Nishiura, and E. Takasugi, PSEUDODIRAC NEUTRINO, *Prog. Theor. Phys.* **70**, 1331 (1983).
- [8] M. Kobayashi and C. S. Lim, Pseudo Dirac scenario for neutrino oscillations, *Phys. Rev. D* **64**, 013003 (2001), [arXiv:hep-ph/0012266](https://arxiv.org/abs/hep-ph/0012266).
- [9] I. Martinez-Soler, Y. F. Perez-Gonzalez, and M. Sen, Signs of pseudo-Dirac neutrinos in SN1987A data, *Phys. Rev. D* **105**, 095019 (2022), [arXiv:2105.12736 \[hep-ph\]](https://arxiv.org/abs/2105.12736).
- [10] K. Carloni, I. Martínez-Soler, C. A. Argüelles, K. S. Babu, and P. S. B. Dev, Probing pseudo-Dirac neutrinos with astrophysical sources at IceCube, *Phys. Rev. D* **109**, L051702 (2024), [arXiv:2212.00737 \[astro-ph.HE\]](https://arxiv.org/abs/2212.00737).
- [11] C. Giunti, C. W. Kim, and U. W. Lee, Oscillations of pseudoDirac neutrinos and the solar neutrino problem, *Phys. Rev. D* **46**, 3034 (1992), [arXiv:hep-ph/9205214](https://arxiv.org/abs/hep-ph/9205214).
- [12] M. Cirelli, G. Marandella, A. Strumia, and F. Vissani, Probing oscillations into sterile neutrinos with cosmology, astrophysics and experiments, *Nucl. Phys. B* **708**, 215 (2005), [arXiv:hep-ph/0403158](https://arxiv.org/abs/hep-ph/0403158).
- [13] A. de Gouvea, W.-C. Huang, and J. Jenkins, Pseudo-Dirac Neutrinos in the New Standard Model, *Phys. Rev. D* **80**, 073007 (2009), [arXiv:0906.1611 \[hep-ph\]](https://arxiv.org/abs/0906.1611).
- [14] G. Anamiati, R. M. Fonseca, and M. Hirsch, Quasi Dirac neutrino oscillations, *Phys. Rev. D* **97**, 095008 (2018), [arXiv:1710.06249 \[hep-ph\]](https://arxiv.org/abs/1710.06249).
- [15] A. de Gouvêa, E. McGinness, I. Martinez-Soler, and Y. F. Perez-Gonzalez, pp solar neutrinos at DARWIN, *Phys. Rev. D* **106**, 096017 (2022), [arXiv:2111.02421 \[hep-ph\]](https://arxiv.org/abs/2111.02421).

- [16] S. Ansarifard and Y. Farzan, Revisiting pseudo-Dirac neutrino scenario after recent solar neutrino data, *Phys. Rev. D* **107**, 075029 (2023), arXiv:2211.09105 [hep-ph].
- [17] J. Franklin, Y. F. Perez-Gonzalez, and J. Turner, JUNO as a probe of the pseudo-Dirac nature using solar neutrinos, *Phys. Rev. D* **108**, 035010 (2023), arXiv:2304.05418 [hep-ph].
- [18] A. De Gouvêa, I. Martinez-Soler, Y. F. Perez-Gonzalez, and M. Sen, Fundamental physics with the diffuse supernova background neutrinos, *Phys. Rev. D* **102**, 123012 (2020), arXiv:2007.13748 [hep-ph].
- [19] R. M. Crocker, F. Melia, and R. R. Volkas, Oscillating Neutrinos from the Galactic Center, *Astrophys. J. Suppl. Ser.* **130**, 339 (2000), arXiv:astro-ph/9911292 [astro-ph].
- [20] R. M. Crocker, F. Melia, and R. R. Volkas, Searching for Long-Wavelength Neutrino Oscillations in the Distorted Neutrino Spectrum of Galactic Supernova Remnants, *Astrophys. J. Suppl. Ser.* **141**, 147 (2002), arXiv:astro-ph/0106090 [astro-ph].
- [21] J. F. Beacom, N. F. Bell, D. Hooper, J. G. Learned, S. Pakvasa, and T. J. Weiler, PseudoDirac neutrinos: A Challenge for neutrino telescopes, *Phys. Rev. Lett.* **92**, 011101 (2004), arXiv:hep-ph/0307151.
- [22] P. Keranen, J. Maalampi, M. Myrskylainen, and J. Riitinen, Effects of sterile neutrinos on the ultrahigh-energy cosmic neutrino flux, *Phys. Lett. B* **574**, 162 (2003), arXiv:hep-ph/0307041.
- [23] A. Esmaili, Pseudo-Dirac Neutrino Scenario: Cosmic Neutrinos at Neutrino Telescopes, *Phys. Rev. D* **81**, 013006 (2010), arXiv:0909.5410 [hep-ph].
- [24] A. Esmaili and Y. Farzan, Implications of the Pseudo-Dirac Scenario for Ultra High Energy Neutrinos from GRBs, *JCAP* **12**, 014, arXiv:1208.6012 [hep-ph].
- [25] A. S. Joshipura, S. Mohanty, and S. Pakvasa, Pseudo-Dirac neutrinos via a mirror world and depletion of ultrahigh energy neutrinos, *Phys. Rev. D* **89**, 033003 (2014), arXiv:1307.5712 [hep-ph].
- [26] I. M. Shoemaker and K. Murase, Probing BSM Neutrino Physics with Flavor and Spectral Distortions: Prospects for Future High-Energy Neutrino Telescopes, *Phys. Rev. D* **93**, 085004 (2016), arXiv:1512.07228 [astro-ph.HE].
- [27] V. Brdar and R. S. L. Hansen, IceCube Flavor Ratios with Identified Astrophysical Sources: Towards Improving New Physics Testability, *JCAP* **02**, 023, arXiv:1812.05541 [hep-ph].
- [28] C. S. Fong and Y. Porto, Constraining pseudo-Diracness with astrophysical neutrino flavors, (2024), arXiv:2406.15566 [hep-ph].
- [29] P. S. B. Dev, P. A. N. Machado, and I. Martinez-Soler, Pseudo-Dirac neutrinos and relic neutrino matter effect on the high-energy neutrino flavor composition, *Phys. Lett. B* **862**, 139306 (2025), arXiv:2406.18507 [hep-ph].
- [30] Y. F. Perez-Gonzalez and M. Sen, From Dirac to Majorana: The cosmic neutrino background capture rate in the minimally extended Standard Model, *Phys. Rev. D* **109**, 023022 (2024), arXiv:2308.05147 [hep-ph].
- [31] R. Barbieri and A. Dolgov, Bounds on Sterile-neutrinos from Nucleosynthesis, *Phys. Lett. B* **237**, 440 (1990).
- [32] K. Enqvist, K. Kainulainen, and J. Maalampi, Resonant neutrino transitions and nucleosynthesis, *Phys. Lett. B* **249**, 531 (1990).
- [33] Z. Chen, J. Liao, J. Ling, and B. Yue, Constraining superlight sterile neutrinos at Borexino and KamLAND, *JHEP* **09**, 004, arXiv:2205.07574 [hep-ph].
- [34] R. Abbasi *et al.* (IceCube), Evidence for neutrino emission from the nearby active galaxy NGC 1068, *Science* **378**, 538 (2022), arXiv:2211.09972 [astro-ph.HE].
- [35] T. Rink and M. Sen, Constraints on pseudo-Dirac neutrinos using high-energy neutrinos from NGC 1068, *Phys. Lett. B* **851**, 138558 (2024), arXiv:2211.16520 [hep-ph].
- [36] K. Dixit, L. S. Miranda, and S. Razzaque, Searching for Pseudo-Dirac neutrinos from Astrophysical sources in IceCube data (2024), arXiv:2406.06476 [astro-ph.HE].
- [37] M. G. Aartsen *et al.* (IceCube), Evidence for High-Energy Extraterrestrial Neutrinos at the IceCube Detector, *Science* **342**, 1242856 (2013), arXiv:1311.5238 [astro-ph.HE].
- [38] M. G. Aartsen *et al.* (IceCube), Observation of High-Energy Astrophysical Neutrinos in Three Years of IceCube Data, *Phys. Rev. Lett.* **113**, 101101 (2014), arXiv:1405.5303 [astro-ph.HE].
- [39] R. Abbasi *et al.* (IceCube), The IceCube high-energy starting event sample: Description and flux characterization with 7.5 years of data, *Phys. Rev. D* **104**, 022002 (2021), arXiv:2011.03545 [astro-ph.HE].
- [40] M. G. Aartsen *et al.* (IceCube), Atmospheric and astrophysical neutrinos above 1 TeV interacting in IceCube, *Phys. Rev. D* **91**, 022001 (2015), arXiv:1410.1749 [astro-ph.HE].
- [41] M. G. Aartsen *et al.* (IceCube), A combined maximum-likelihood analysis of the high-energy astrophysical neutrino flux measured with IceCube, *Astrophys. J.* **809**, 98 (2015), arXiv:1507.03991 [astro-ph.HE].
- [42] M. G. Aartsen *et al.* (IceCube), Characteristics of the diffuse astrophysical electron and tau neutrino flux with six years of IceCube high energy cascade data, *Phys. Rev. Lett.* **125**, 121104 (2020), arXiv:2001.09520 [astro-ph.HE].
- [43] R. Abbasi *et al.* (IceCube), Characterization of the astrophysical diffuse neutrino flux using starting track events in IceCube, *Phys. Rev. D* **110**, 022001 (2024), arXiv:2402.18026 [astro-ph.HE].
- [44] M. G. Aartsen *et al.* (IceCube), Evidence for Astrophysical Muon Neutrinos from the Northern Sky with IceCube, *Phys. Rev. Lett.* **115**, 081102 (2015), arXiv:1507.04005 [astro-ph.HE].
- [45] M. G. Aartsen *et al.* (IceCube), Observation and Characterization of a Cosmic Muon Neutrino Flux from the Northern Hemisphere using six years of IceCube data, *Astrophys. J.* **833**, 3 (2016), arXiv:1607.08006 [astro-ph.HE].
- [46] R. Abbasi *et al.*, Improved Characterization of the Astrophysical Muon-neutrino Flux with 9.5 Years of IceCube Data, *Astrophys. J.* **928**, 50 (2022), arXiv:2111.10299 [astro-ph.HE].
- [47] For other explanations of the track-vs-cascade tension in the previous IceCube data, see e.g., Refs. [67–70].
- [48] H. Yuksel, M. D. Kistler, J. F. Beacom, and A. M. Hopkins, Revealing the High-Redshift Star Formation Rate with Gamma-Ray Bursts, *Astrophys. J. Lett.* **683**, L5 (2008), arXiv:0804.4008 [astro-ph].
- [49] M. Elías-Chávez and O. M. Martínez, Estimation of the Star Formation Rate using Long-Gamma Ray Burst observed by SWIFT, *Rev. Mex. Astron. Astrofis.* **54**, 309 (2018), arXiv:2006.03367 [astro-ph.GA].
- [50] D. Chang and O. C. W. Kong, Pseudo-Dirac neutrinos, *Phys. Lett. B* **477**, 416 (2000), arXiv:hep-ph/9912268.
- [51] Y. Nir, PseudoDirac solar neutrinos, *JHEP* **06**, 039,

arXiv:hep-ph/0002168.

- [52] A. S. Joshipura and S. D. Rindani, Phenomenology of pseudoDirac neutrinos, *Phys. Lett. B* **494**, 114 (2000), arXiv:hep-ph/0007334.
- [53] M. Lindner, T. Ohlsson, and G. Seidl, Seesaw mechanisms for Dirac and Majorana neutrino masses, *Phys. Rev. D* **65**, 053014 (2002), arXiv:hep-ph/0109264.
- [54] K. R. S. Balaji, A. Kalliomaki, and J. Maalampi, Revisiting pseudoDirac neutrinos, *Phys. Lett. B* **524**, 153 (2002), arXiv:hep-ph/0110314.
- [55] G. J. Stephenson, Jr., J. T. Goldman, B. H. J. McKellar, and M. Garbutt, Large mixing from small: PseudoDirac neutrinos and the singular seesaw, *Int. J. Mod. Phys. A* **20**, 6373 (2005), arXiv:hep-ph/0404015.
- [56] K. L. McDonald and B. H. J. McKellar, The Type-II Singular See-Saw Mechanism, *Int. J. Mod. Phys. A* **22**, 2211 (2007), arXiv:hep-ph/0401073.
- [57] Y. H. Ahn, S. K. Kang, and C. S. Kim, A Model for Pseudo-Dirac Neutrinos: Leptogenesis and Ultra-High Energy Neutrinos, *JHEP* **10**, 092, arXiv:1602.05276 [hep-ph].
- [58] K. S. Babu, X.-G. He, M. Su, and A. Thapa, Naturally light Dirac and pseudo-Dirac neutrinos from left-right symmetry, *JHEP* **08**, 140, arXiv:2205.09127 [hep-ph].
- [59] H. Ooguri and C. Vafa, Non-supersymmetric AdS and the Swampland, *Adv. Theor. Math. Phys.* **21**, 1787 (2017), arXiv:1610.01533 [hep-th].
- [60] L. E. Ibanez, V. Martin-Lozano, and I. Valenzuela, Constraining Neutrino Masses, the Cosmological Constant and BSM Physics from the Weak Gravity Conjecture, *JHEP* **11**, 066, arXiv:1706.05392 [hep-th].
- [61] E. Gonzalo, L. E. Ibáñez, and I. Valenzuela, Swampland constraints on neutrino masses, *JHEP* **02**, 088, arXiv:2109.10961 [hep-th].
- [62] G. F. Casas, L. E. Ibáñez, and F. Marchesano, On small Dirac neutrino masses in string theory, *JHEP* **01**, 083, arXiv:2406.14609 [hep-th].
- [63] C. S. Fong, T. Gregoire, and A. Tonero, Testing quasi-Dirac leptogenesis through neutrino oscillations, *Phys. Lett. B* **816**, 136175 (2021), arXiv:2007.09158 [hep-ph].
- [64] M. Chianese, P. Di Bari, K. Farrag, and R. Samanta, Probing relic neutrino radiative decays with 21 cm cosmology, *Phys. Lett. B* **790**, 64 (2019), arXiv:1805.11717 [hep-ph].
- [65] P. S. B. Dev, P. Di Bari, I. Martínez-Soler, and R. Roshan, Relic neutrino decay solution to the excess radio background, *JCAP* **04**, 046, arXiv:2312.03082 [hep-ph].
- [66] Note that, unlike standard oscillatory terms, quasi-Dirac oscillations are not necessarily washed out by extragalactic baselines. This is because the coherence length is

$$L_{\text{coh}} = \frac{4\sqrt{2}E^2}{|\delta m_k^2|} \sigma_x$$

$$\approx 18 \text{ Gpc} \left(\frac{E}{10 \text{ TeV}} \right)^2 \left(\frac{10^{-19} \text{ eV}^2}{\delta m_k^2} \right) \left(\frac{\sigma_x}{10^{-19} \text{ m}} \right).$$

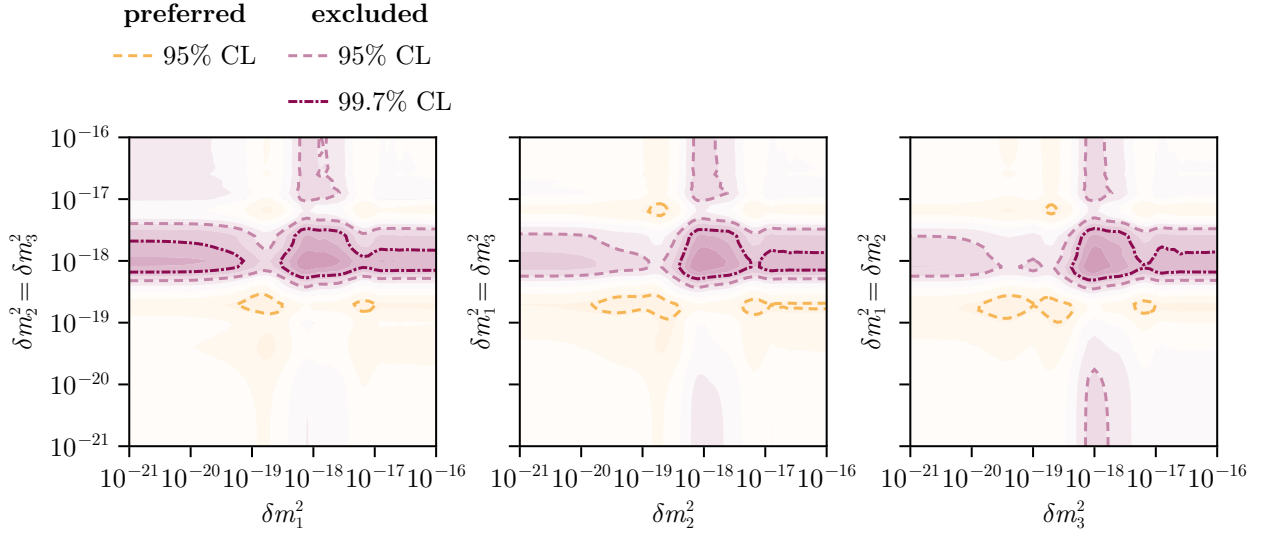
Therefore, for benchmark values of 10 TeV and $\delta m_k^2 = 10^{-19} \text{ eV}^2$, the coherence length is comparable to the radius of the observable universe, even for the size of the wavepacket $\sigma_x \sim 10^{-19} \text{ m}$, orders of magnitude smaller than the smallest wave packets ever considered [71].

- [67] Y. Sui and P. S. B. Dev, A Combined Astrophys-

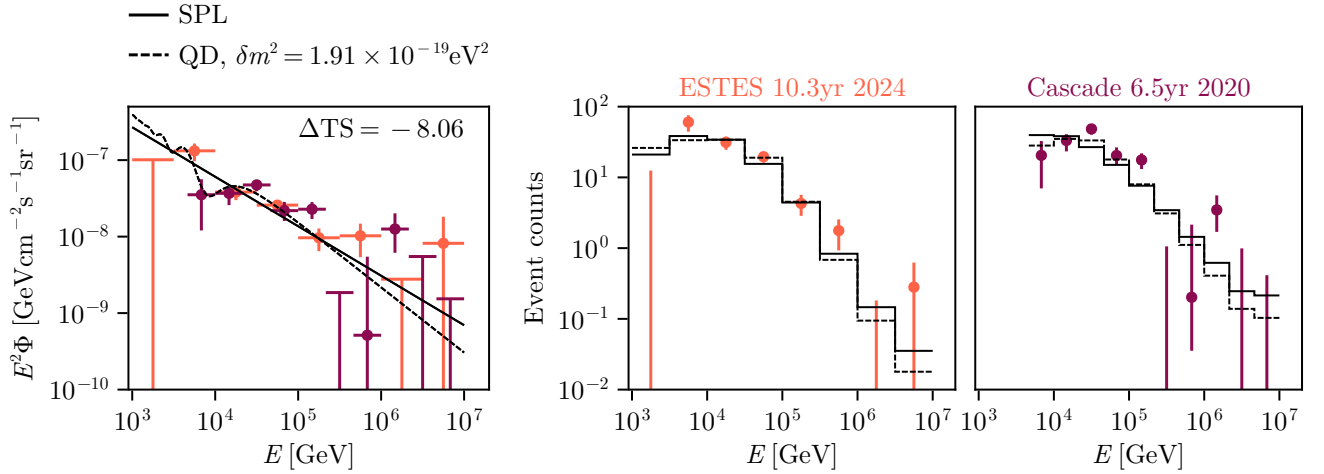
ical and Dark Matter Interpretation of the IceCube HESE and Throughgoing Muon Events, *JCAP* **07**, 020, arXiv:1804.04919 [hep-ph].

- [68] A. Palladino, The flavor composition of astrophysical neutrinos after 8 years of IceCube: an indication of neutron decay scenario?, *Eur. Phys. J. C* **79**, 500 (2019), arXiv:1902.08630 [astro-ph.HE].
- [69] A. Abdullahi and P. B. Denton, Visible Decay of Astrophysical Neutrinos at IceCube, *Phys. Rev. D* **102**, 023018 (2020), arXiv:2005.07200 [hep-ph].
- [70] L. M. G. de la Vega, E. Peinado, and J. Wudka, $L\mu-L\tau$ solution to the IceCube ultrahigh-energy neutrino deficit in light of NA64, *Phys. Rev. D* **110**, 095032 (2024), arXiv:2406.19968 [hep-ph].
- [71] J. Kersten and A. Y. Smirnov, Decoherence and oscillations of supernova neutrinos, *Eur. Phys. J. C* **76**, 339 (2016), arXiv:1512.09068 [hep-ph].

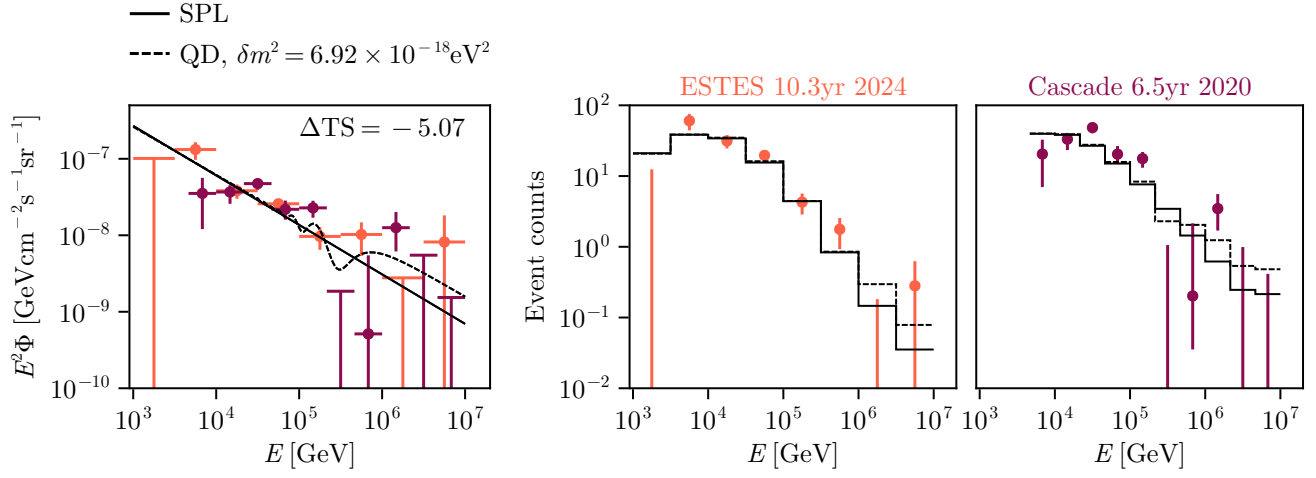
Supplemental Material



SUPPL. FIG. 1. Constraints on two-parameter QDino models in which two generations have the same hyperfine mass-squared splittings. From left to right, we plot $\delta m_2^2 = \delta m_3^2$, $\delta m_1^2 = \delta m_3^2$, and $\delta m_1^2 = \delta m_2^2$.



SUPPL. FIG. 2. Flux models and corresponding event distributions, for the best-fit single power law and QDino hypotheses. The QDino scenario assumes equal mass-squared differences $\delta m_k^2 = \delta m^2$.



SUPPL. FIG. 3. Flux models and corresponding event distributions, for the best-fit SPL and second-best QDino hypotheses.